

High-field study of normal-state magnetotransport in $\text{Ti}_2\text{Ba}_2\text{CuO}_{6+\delta}$

A. W. Tyler*

IRC in Superconductivity, Madingley Road, Cambridge, CB3 0HE, United Kingdom

Yoichi Ando[†]

Bell Laboratories, Lucent Technologies, 700 Mountain Avenue, Murray Hill, New Jersey 07974

F. F. Balakirev

Bell Laboratories, Lucent Technologies, 700 Mountain Avenue, Murray Hill, New Jersey 07974

and Los Alamos National Laboratory, MS E534, Los Alamos, New Mexico 87545

A. Passner

Bell Laboratories, Lucent Technologies, 700 Mountain Avenue, Murray Hill, New Jersey 07974

G. S. Boebinger

Bell Laboratories, Lucent Technologies, 700 Mountain Avenue, Murray Hill, New Jersey 07974

and Los Alamos National Laboratory, MS E534, Los Alamos, New Mexico 87545

A. J. Schofield

T.C.M., Cavendish Laboratory, Madingley Road, Cambridge, CB3 0HE, United Kingdom

A. P. Mackenzie*

IRC in Superconductivity, Madingley Road, Cambridge, CB3 0HE, United Kingdom

O. Laborde

Centre de Recherche sur les Très Basses Températures, Laboratoire des Champs Magnétiques Intenses, CNRS Boîte Postale 166, 38042 Grenoble-cédex, France

(Received 1 October 1997)

We present a study of in-plane normal-state magnetotransport in single-crystal $\text{Ti}_2\text{Ba}_2\text{CuO}_{6+\delta}$ in 60-T pulsed magnetic fields. In optimally doped samples ($T_c \sim 80$ K) the weak-magnetic-field regime extends to fields as high as 60 T, but in overdoped samples ($T_c \sim 30$ K) we are able to leave the weak-field regime, as shown by the behavior of both the magnetoresistance and the Hall resistance. Data from samples of both dopings provide constraints on the class of model necessary to describe normal-state transport in the cuprates. [S0163-1829(98)50602-9]

Measurements of the electrical transport properties of the high- T_c cuprate superconductors have proved to be one of the most useful ways of probing their anomalous normal-state properties. Studies of the Hall effect in $\text{YBa}_2\text{Cu}_3\text{O}_{7-\delta}$ (Ref. 1) show that near optimum doping, the resistivity (ρ) has an approximately linear temperature dependence, while the inverse Hall angle ($\cot \theta_H$) varies nearly quadratically with temperature. Systematic measurements of these properties have been made in many cuprate materials, as a function of disorder and carrier concentration. Although some exceptions have been reported, the experimental picture which has emerged is that $\cot \theta_H$ continues to vary approximately quadratically in temperature even when ρ changes its temperature dependence from linear on underdoping or overdoping.

Most attempts to understand this intriguing behavior fall into two broad classes. In the first (the “two-lifetime” models), the experimental observations are taken to indicate the existence of two separate and essentially decoupled scattering times governing longitudinal transport and Hall transport, often referred to as τ_{lr} and τ_H , respectively.^{2,3} These two intrinsic lifetimes are assumed to coexist at all points on the Fermi surface (FS). Theories constructed from this start-

ing point are intrinsically non-Fermi-liquid in nature. The more conventional class of models (the “anisotropic” models) exploits the fourfold anisotropy of the cuprate Fermi surfaces and postulates the existence of an anisotropic scattering rate whose magnitude and temperature dependence is different on different parts of the FS.⁴⁻⁶

To date, almost all normal-state magnetotransport studies on the cuprates have been performed in magnetic fields of less than 20 T, in the weak-field regime ($\omega_c \tau \ll 1$, where ω_c is the cyclotron frequency and τ^{-1} is the scattering rate). In this regime, the magnetoresistance is parabolic in B ,⁷⁻¹⁰ and the Hall voltage is linear in B . Recently, Harris *et al.*⁷ pointed out that the magnitude of the weak-field (“WF”) orbital normal-state magnetoresistance (MR) ($\Delta\rho/\rho^{WF}$) is proportional to the variation of the local Hall angle around the Fermi surface. Observations on $\text{YBa}_2\text{Cu}_3\text{O}_{7-\delta}$ and optimally doped $\text{La}_{2-x}\text{Sr}_x\text{CuO}_4$ have shown that the temperature dependence of the MR agrees with that of the square of the Hall angle, favoring two-lifetime models for which τ_H exists at all points on the FS.⁷

Here, we report magnetotransport results on single crystals of $\text{Ti}_2\text{Ba}_2\text{CuO}_{6+\delta}$ in 60-T pulsed magnetic fields. In

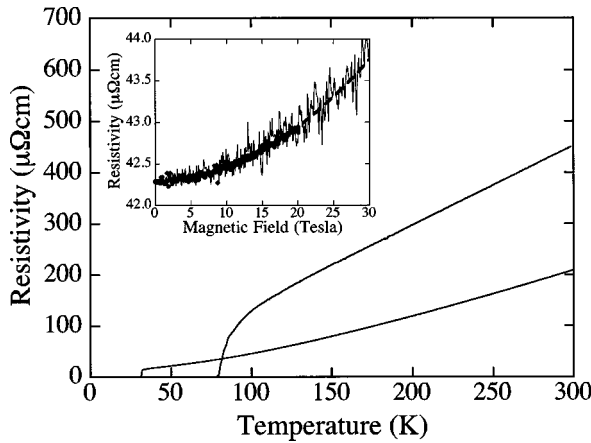


FIG. 1. The resistivity in zero magnetic field of optimally doped ($T_c \sim 80$ K) and overdoped ($T_c \sim 30$ K) single crystals of $\text{Ti}_2\text{Ba}_2\text{CuO}_{6+\delta}$. The inset shows a comparison of magnetoresistance (MR) measurements in dc (circles) and pulsed (solid line) magnetic fields at $T \sim 115$ K for an overdoped sample. The MR in this range can be well fitted with a quadratic field dependence (dashed line). The pulsed field MR data were multiplied by a factor of 1.015 to correct for a small difference in the temperature at which the pulsed and dc measurements were made.

samples near optimum doping ($T_c \sim 80$ K), the weak-field regime is seen to extend to nearly 60 T, and we see behavior similar to that observed in $\text{YBa}_2\text{Cu}_3\text{O}_{7-\delta}$ and optimally doped $\text{La}_{2-x}\text{Sr}_x\text{CuO}_4$. In strongly overdoped samples ($T_c \sim 30$ K), however, we are able to observe significant deviations from the weak-field forms of $\rho_{xx}(B)$ and $\rho_{xy}(B)$. We find that the high-field magnetotransport provides an independent way of estimating an important parameter, $\omega_c\tau$, and thus provides additional constraints to the existing transport models.

Tetragonal single crystals of $\text{Ti}_2\text{Ba}_2\text{CuO}_{6+\delta}$ were grown using a Cu-rich flux. With $\text{Ti}_2\text{Ba}_2\text{CuO}_{6+\delta}$ degradation of the surface quality on annealing is a persistent problem, leading to poor quality electrical contacts for the transport measurements. In our experience, the best way of making contacts to samples with elevated T_c is to evaporate gold contact pads onto the as-grown sample. The desired T_c values were then achieved by annealing using various combinations of annealing temperature, atmosphere, and time. The anneal also diffuses the gold into the sample, providing a low-resistance contact to which gold wires are attached using a silver paint (Dupont 4929) which hardens in air at room temperature. Care was taken when evaporating the gold to ensure that it covered the sides of the sample. The resistivity for optimal ($T_c \sim 80$ K) and overdoped ($T_c \sim 30$ K) samples is shown in Fig. 1.

A resistive dc magnet in Grenoble was used for MR measurements in fields up to 20 T, using a standard four terminal ac technique with a 32 Hz excitation frequency. Temperature stability of 1 part in 10^4 was achieved using a capacitance sensor which is insensitive to field. The temperature was measured in zero field before and after each sweep, to check for possible temperature drift. The longitudinal MR was also measured at several temperatures and found to be at most 5% of the total MR. The total measured transverse MR is thus dominated by the orbital MR for all of the data in the figures.

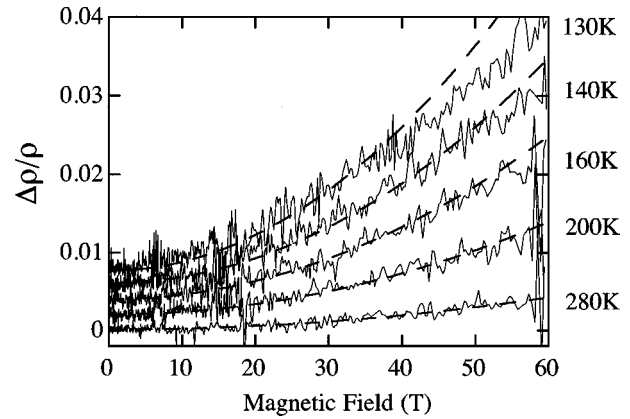


FIG. 2. The MR of an optimally doped crystal of $\text{Ti}_2\text{Ba}_2\text{CuO}_{6+\delta}$ ($T_c \sim 80$ K) at a series of temperatures between 130 and 280 K. Data at different temperatures have been offset for ease of viewing. The dashed lines are parabolic fits to the data.

Precise measurement of normal-state magnetotransport in a pulsed field presented a considerable challenge, due to the higher noise levels and the relatively low resistances of the $\text{Ti}_2\text{Ba}_2\text{CuO}_{6+\delta}$ crystals (as little as 10 mΩ below 50 K). After some experimentation, voltage sensitivity of better than 1 μV could be achieved at excitation currents of 5–10 mA. The temperature was stabilized and measured in zero field. Comparison of up- and down-sweeps was used to check for eddy current heating, which was largely avoided due to the very small sample sizes (typically $300 \times 100 \times 15 \mu\text{m}^3$). Also, all the data shown in this paper are at sufficiently high temperatures that the MR is dominated by normal-state orbital contributions rather than superconducting fluctuations.

Given the difficulty of using a pulsed field to measure small MR effects in low-resistance samples, we first established, using four different samples, that the results using dc and pulsed techniques are consistent. As an example, in the inset to Fig. 1 we show the resistivity at 115 K of one of the overdoped samples measured as a function of magnetic field up to 20 T in the resistive dc field (circles). The data measured in the pulsed magnetic field at Bell Labs (solid line) overlays the dc field data very well.

Figure 2 contains pulsed field MR data from a sample near optimal doping ($T_c \sim 80$ K). For this sample, the MR is small (only 3% at 60 T and 130 K) and the field dependence is basically quadratic for $T > 130$ K (dashed line in the figure) over the whole field range. This is good evidence that the weak-field regime is applicable in fields as high as 60 T in optimally doped $\text{Ti}_2\text{Ba}_2\text{CuO}_{6+\delta}$.

Since a single isotropic band has zero MR, the parabolic MR in Fig. 2 might result from anisotropy, whether the scattering rate varies around the FS (Refs. 4–6) or the “local cyclotron effective mass” m^* (proportional to $1/v_F$) varies due to the local geometry of the FS.⁷ Interestingly, it is also possible to construct two-lifetime models in which neither τ nor m^* are anisotropic, yet there is a nonzero MR. In one such model,³ fast and slow relaxation rates exist at all \mathbf{k} points. In terms of the MR, this is roughly analogous to a two-fluid picture, and a quadratic weak-field MR results even for a parabolic band. Thus, the model-specific part of the

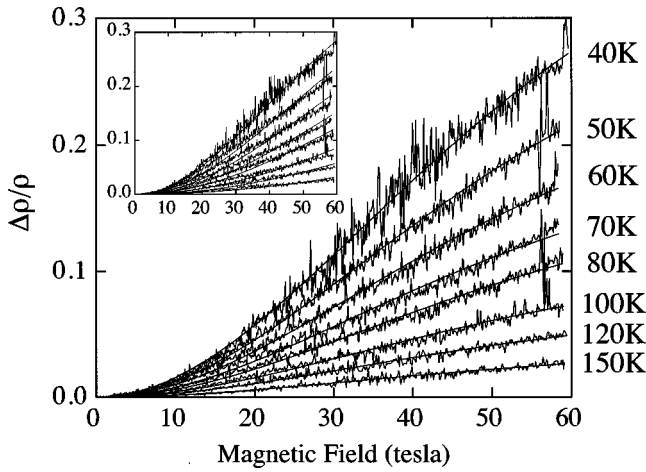


FIG. 3. The MR of an overdoped crystal of $\text{Ti}_2\text{Ba}_2\text{CuO}_{6+\delta}$ ($T_c \sim 30$ K) at a series of temperatures between 40 and 150 K. The fits (solid lines) are produced by a general expression for orbital MR beyond the weak-field limit [Eq. (1)]. The inset shows the same data fitted to Eq. (2) with $\omega_c\tau_{tr}$ fixed by the resistivity data of Fig. 1.

data in Fig. 2 is not the parabolicity, $\Delta\rho/\rho^{WF} = \alpha B^2$, rather it is the interpretation of the prefactor α in terms of the lifetimes (or masses).

At optimal doping, the Hall effect in $\text{Ti}_2\text{Ba}_2\text{CuO}_{6+\delta}$ gives a very clear example of two-lifetime behavior, with ρ and $\cot\theta_H$ following linear and quadratic temperature dependences to an accuracy that poses a challenge to any theory of the cuprate normal state.¹¹ Harris *et al.*⁷ have shown that in $\text{YBa}_2\text{Cu}_3\text{O}_{7-\delta}$ and $\text{La}_{2-x}\text{Sr}_x\text{CuO}_4$ near optimal doping, the weak field MR obeys a special form of Kohler's rule in which $(\cot\theta_H)^2\Delta\rho/\rho$ scale at different temperatures, while the traditional Kohler scaling $\rho\Delta\rho/B^2$ is violated. This is also the case for the MR data from the optimally doped $\text{Ti}_2\text{Ba}_2\text{CuO}_{6+\delta}$ of Fig. 2. As discussed in Ref. 7 and above, this observation favors two-lifetime models in which lifetimes with two different temperature dependences exist at all points of the FS.

Because the 60-T magnetic field reveals a strictly parabolic MR in the optimally doped sample, we turn our attention to overdoped samples with lower resistivity to better reach the high-magnetic-field regime. The MR of the overdoped samples is much larger, and deviates significantly from a quadratic field dependence at high fields and low temperatures. Going beyond the weak-field limit in any of the models discussed above leads to a modified general expression of the form

$$\frac{\Delta\rho}{\rho} = \frac{\alpha B^2}{1 + (\beta B)^2}, \quad (1)$$

where β is a second constant, principally related to the overall scale of $\omega_c\tau$. This expression accounts for the data in Fig. 3 quite well, as shown by the curve fits, so our observations are consistent with the onset of MR saturation as we leave the weak-field regime.¹²

To determine whether high-field MR can constrain which general class of models is applicable to the cuprates, we examine the physical origin of weak- and strong-field MR in more detail. As discussed above, in conventional models, the

weak-field MR is a measure of anisotropy around the FS, although its magnitude is not easy to interpret. However, saturation is much easier to interpret, because it arises once the quasiparticles orbit a significant fraction of the Fermi surface between scattering events. Thus $\beta \sim e\langle m^*/\tau \rangle^{-1}$, where τ is the scattering lifetime and $\langle \rangle$ denotes a FS average. The product βB gives the value of $\omega_c\tau$ determined from the high-field MR.

The different classes of model for the cuprate normal state make very different predictions for the relationship between this high-field value of $\omega_c\tau$ and those that can be estimated from the resistivity and weak-field Hall effect. If the Hall effect and resistivity are to be understood in terms of an anisotropic model,⁴⁻⁶ the fast and slow relaxation rates which lead to τ_{tr} and τ_H exist on different parts of the FS.¹³ When $\omega_c\tau_{tr}$ is estimated from ρ and $\omega_c\tau_H$ is estimated from θ_H , we find that $\omega_c\tau_H > \omega_c\tau_{tr}$ for all temperatures below room temperature. Since high-field MR saturation would be expected to be controlled by those regions with the highest scattering rate, the value of $\omega_c\tau$ estimated from high-field MR would be expected to be close to $\omega_c\tau_{tr}$ (and not to $\omega_c\tau_H$). We shall show that this is apparently not the case for our data.¹⁴

The opposite conclusion, that the high-field MR is determined by $\omega_c\tau_H$, is reached for two-lifetime models, two of which we shall consider here. In the picture discussed in Refs. 1, 2, and 7, τ_H governs all responses to a magnetic field. Since τ_H is constant around the FS in this model, some v_F anisotropy is necessary for the appearance of a nonzero MR. Models of the FS of $\text{Ti}_2\text{Ba}_2\text{CuO}_{6+\delta}$ show that v_F is smallest in the regions of highest FS curvature,¹⁵ so the high-field MR would be expected to give $\omega_c\tau$ with the temperature dependence of τ_H and a magnitude which is determined primarily by the curved parts of the FS. Since a weak-field measurement of the Hall angle contains an even stronger weighting to areas of large FS curvature,¹⁶ the value of $\omega_c\tau$ obtained from high-field measurements would be expected to be similar to that determined from weak-field Hall measurements at all temperatures.

In the formulation of a two-lifetime model described in Ref. 3, a simple analytical expression can be derived for the MR in terms of the quantities $\omega_c\tau_{tr}$ and $\omega_c\tau_H$, if FS anisotropy is neglected:

$$\frac{\Delta\rho}{\rho} = \frac{\omega_c\tau_H(\omega_c\tau_H - \omega_c\tau_{tr})}{(1 + \omega_c^2\tau_H^2)}. \quad (2)$$

In both two-lifetime models, then, high-field saturation is expected to probe $\omega_c\tau_H$. Our data support this expectation. The value of β fitted from the data at 40 K where the saturation is largest corresponds to $\omega_c\tau$ of 0.9 at 60 T. At that temperature the weak-field Hall angle per tesla is 0.01 T^{-1} giving an estimated value for $\omega_c\tau_H$ of 0.6 at 60 T. The measured ρ can be used to estimate $\omega_c\tau_{tr}$ for a large FS [corresponding to $k_F \sim 0.7 \text{ \AA}^{-1}$ (Ref. 17)] using the expression $\omega_c\tau_{tr} = 2\pi dB/e k_F^2 \rho$, where d is the interplane spacing of 11.6 \AA . At 60 T, $\omega_c\tau_{tr}$ is only 0.3, so the MR value for $\omega_c\tau$ derived from high fields certainly seems to be in better agreement with $\omega_c\tau_H$.

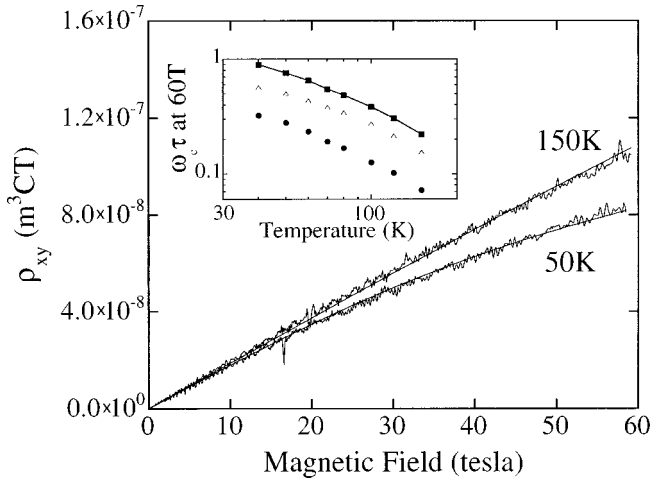


FIG. 4. The Hall resistivity ρ_{xy} for the $T_c \sim 30$ K crystal at 50 and 150 K. The fits (solid lines) to Eq. (3) were made with both $\omega_c \tau_{lr}$ and $\omega_c \tau_H$ fixed by the fits to the MR data in Fig. 3. The inset shows the value of $\omega_c \tau_H$ obtained using this procedure (squares joined by solid line) compared with measurements of $\omega_c \tau_H$ from the weak-field Hall angle (triangles) and $\omega_c \tau_{lr}$ from the resistivity (circles).

In the model of Ref. 3, it is also possible to derive an analytical expression for the Hall resistivity

$$\rho_{xy} = \frac{m^* \omega_c}{n e^2} \frac{\omega_c \tau_H}{\omega_c \tau_{lr}} \frac{(1 + \omega_c^2 \tau_H \tau_{lr})}{(1 + \omega_c^2 \tau_H^2)}, \quad (3)$$

where n is the carrier concentration. If we neglect the mild v_F anisotropy round the FS that probably exists, we can reduce Eq. (2) to a single parameter fit for $\omega_c \tau_H$ by estimating $\omega_c \tau_{lr}$ at each temperature from the resistivity data of Fig. 1. The resulting fits are shown in the inset of Fig. 3. Using these values for $\omega_c \tau_H$, fits using Eq. (3) are reduced to a single free parameter: an overall scale factor related to n .

The ρ_{xy} data of Fig. 4 are fitted using Eq. (3) with both $\omega_c \tau_{lr}$ and $\omega_c \tau_H$ fixed. The constrained fits to the MR data are poorer than those in the main panel of Fig. 3 (possibly because of our neglect of the anisotropy), but the fits to ρ_{xy} are very good.

In the inset to Fig. 4, we show the fitted values of $\omega_c \tau_H$ (solid line), along with the values of $\omega_c \tau_{lr}$ (circles) that were used to constrain the fits. Also included are the values of $\omega_c \tau_H$ (triangles) obtained from the weak-field Hall angle. Again, we find that the scattering time determined from the high-field MR agrees better with the τ_H determined from the weak-field Hall angle than with the τ_{lr} determined from the resistivity.

Given the approximations used, we do not claim to favor the particular two-lifetime model of Eqs. (2) and (3). Rather, the combination of data from the weak-field regime in the optimally doped sample and the high-field regime for the overdoped sample does appear to favor some kind of two-lifetime model for the cuprate normal state. It would be very interesting to analyze high-field MR saturation in cuprates at optimal doping, where separate temperature dependences of the two scattering times are observed; however, this would require much higher magnetic fields than are currently available.

In summary, we have succeeded in studying normal-state magnetotransport of single-crystal $\text{Ti}_2\text{Ba}_2\text{CuO}_{6+\delta}$ in 60-T pulsed magnetic fields to obtain new constraints on the scattering mechanisms in the cuprates. In optimally doped samples, the weak-magnetic-field regime reaches to fields as high as 60 T. In overdoped samples, we leave the weak-field regime, as shown by the behavior of both the MR and the Hall resistance. Analysis of the MR and Hall effect for both the optimally doped and overdoped samples gives evidence in support of those models for the normal state of the cuprates in which two scattering lifetimes exist at all points on the Fermi surface.

*Present address: School of Physics and Astronomy, University of Birmingham, Edgbaston, Birmingham, B15 2TT, United Kingdom.

†Present address: Central Research Institute of Electric Power Industry, Komae, Tokyo 201, Japan.

¹T. R. Chien, Z. Z. Wang, and N. P. Ong, Phys. Rev. Lett. **67**, 2088 (1991).

²P. W. Anderson, Phys. Rev. Lett. **67**, 2092 (1991).

³P. Coleman, A. J. Schofield, and A. M. Tsvelik, Phys. Rev. Lett. **76**, 1324 (1996).

⁴A. Carrington *et al.*, Phys. Rev. Lett. **69**, 2855 (1992).

⁵C. Kendziora *et al.*, Phys. Rev. B **46**, 14 297 (1992).

⁶B. P. Stojković and D. Pines, Phys. Rev. Lett. **76**, 811 (1996); Phys. Rev. B **55**, 8576 (1997).

⁷J. M. Harris *et al.*, Phys. Rev. Lett. **75**, 1391 (1995).

⁸T. Kimura *et al.*, Phys. Rev. B **53**, 8733 (1996).

⁹N. E. Hussey *et al.*, Phys. Rev. Lett. **76**, 122 (1996).

¹⁰F. F. Balakirev *et al.*, cond-mat/9705107 (unpublished).

¹¹A.W. Tyler and A.P. Mackenzie, Physica C **282-287**, 1185 (1997).

¹²Data from the optimally doped sample do show evidence of the high-field regime for $T < 140$ K; however, the deviations from parabolicity are too small to usefully constrain β of Eq. (1). Also, interpretation of $T < 130$ K data is complicated by evidence of superconducting fluctuations.

¹³In some formulations (Refs. 4 and 5), ρ is dominated by scattering on flat parts of a square FS, while in others (Ref. 6) both the Hall effect and resistivity are determined by FS averages of “hot” and “cold” scattering rates which have noninteger power-law temperature dependences.

¹⁴This simple analysis based on the high-field regime ($\omega_c \tau \gg 1$) may become more complicated when applied to the highest field regime ($\omega_c \tau \sim 1$) that we are able to reach in our experiment. B. Stojković and D. Pines (private communication); and (unpublished).

¹⁵D. R. Hamann and L. F. Mattheiss, Phys. Rev. B **38**, 5138 (1988).

¹⁶N. P. Ong, Phys. Rev. B **43**, 193 (1991).

¹⁷A. P. Mackenzie *et al.*, Phys. Rev. B **53**, 5848 (1996).